A Lagrange-multiplier approach for the numerical simulation of an inextensible membrane or thread immersed in a fluid

Jocelyn Etienne, Jérôme Lohéac, Pierre Saramito

A LAGRANGE-MULTIPLIER APPROACH FOR THE NUMERICAL SIMULATION OF AN INEXTENSIBLE MEMBRANE OR THREAD IMMERSED IN A FLUID [*]

JOCELYN ÉTIENNE[†], JÉRÔME LOHÉAC[‡], AND PIERRE SARAMITO[§]

Abstract. The inextensibility constraint is encountered in many physical problems involving thin solids interacting with a fluid. It is generally imposed in numerical simulations by means of a penalty method. Here, we propose a novel saddle-point approach allowing to impose it through a Lagrange multiplier defined on the thin structure, the tension. The functional analysis of the problem allows to determine which boundary conditions are needed for this problem. The forces originating from the structure appear as a boundary condition for the fluid problem, defined on a moving boundary which represents the structure. The problem is discretised with mixed finite elements. The mesh of the thin solid is included in the mesh of the bulk, and is advected by its velocity in the course of time iterations. The appropriate choice of the finite element spaces for this mixed approach is discussed and it is shown that boundary conditions on the thin structure edges impact on this choice. Numerical tests are performed which demonstrate the convergence and robustness of the method. These examples include the simulation of a closed, membrane bound object (a *vesicle*) and of a filament or flag in a large Reynolds-number flow.

Key words. Fluid-structure interactions, surface divergence, saddle-point problem, boundary Lagrange multiplier.

AMS subject classifications. 65M60, 74K05, 74K15, 74F10, 76D05, 76D07

1. Introduction. From sailing to micro-organism swimming, there are innumerable examples of dynamics involving the interactions between a fluid and a thin elastic sheet or a slender filament. Because they are thin or slender, the geometry of these elastic structures introduces a small parameter: the thickness, or the radius, compared to the length. When this parameter is taken to its limit, this problem is a generalisation of interfacial dynamics problems, where the governing equations in the fluid domain are supplemented with a jump boundary condition for the stress at the interface.

An elastic thread is fully characterised by its bending and extension–compression elasticity, while an elastic membrane additionally has a shear elasticity [1]. Here we are interested in the case when the extension–compression modulus is extremely high, that is, of nearly inextensible (and incompressible) threads and membranes. This case is relevant to many physical materials, including most fabric structures such as threads, sails, flags; metal shells such as rods or wings; and biological membranes and flagellae. Some form slender structures (one-dimensional), such as threads, others form thin sheets (two-dimensional), such as flags, leather balls or biological membranes. Another classification is whether the structures are 'closed' such as balls and living cells, or 'open' such as threads, flags, and flagellae.

[†]Université J. Fourier, Grenoble – CNRS, Laboratoire de Spectrométrie Physique, 140 rue de la physique, BP 87, 38402 Saint-Martin-d'Hères Cedex, `Jocelyn.Etienne@UJF-Grenoble.fr`

[‡]Université J. Fourier, Grenoble – CNRS, Laboratoire de Spectrométrie Physique, 140 rue de la physique, BP 87, 38402 Saint-Martin-d'Hères Cedex; Present address: Institut Élie Cartan, UMR 7502, Université Henri Poincaré Nancy 1, B.P. 70239, 54506 Vandoeuvre-lès-Nancy Cedex, `Jerome.Loheac@iecn.u-nancy.fr`

[§]Université J. Fourier, Grenoble – CNRS, Laboratoire Jean Kuntzman, BP 53 – Domaine Universitaire, 38041 Grenoble Cedex, `Pierre.Saramito@imag.fr`

A very high extension modulus makes the problem very ill-conditionned, and not practical for numerical resolution. Two options are available : either to reduce artificially the value of the modulus, but keeping it high, this is the *penalty approach*, or to consider that this modulus is infinite, making the thread totally inextensible, which leads to a *constrained problem*. The penalty approach introduces a parameter, the penalty extension modulus, which needs to be adjusted in simulations to achieve convergence. The numerical result will depend on the penalty modulus. Also, since external forces may vary locally, the actual, non-physical extension of the thread will be higher in regions of strong sollicitation. On the other hand, the constrained problem approach introduces no additional free parameter and imposes inextensibility uniformly. It is thus physically more attractive for approaching very high extension modulus cases, but requires more involved numerical methods.

In this paper we develop a numerical method for the resolution of this constrained problem. The augmented Lagrangian approach of Fortin and Glowinski [2] is widely used for solving problems subject to a constraint, such as volume incompressibility in Stokes and Navier–Stokes equations. Its application to the case of an inextensible thread or membrane immersed in a fluid is described in section 2. A saddle-point approach allows us to characterise the solution in a weak formulation, which is discretised using mixed finite elements in section 3. The choice of finite-element discrete spaces is discussed. Numerical experiments validate the method in section 4, where simulations of both 'closed' membrane-bound objects and 'open' threads with a 'free' endpoint are presented, both in Stokes and high-Reynolds number Navier-Stokes flows.

2. Governing equations and saddle-point approach. Consider a two dimensional domain Ω and a curve $\Gamma_0 = \{\boldsymbol{\gamma}_0(s),\ s \in (0,1)\} \subset \Omega$. This is the initial geometry of the problem, the curve $\Gamma(t) = \{\boldsymbol{\gamma}(t,s),\ s \in (0,1)\} \subset \Omega$ being one of its unknowns, with $\boldsymbol{\gamma}(0,s) = \boldsymbol{\gamma}_0(s)$, and represents the thread immersed in a two-dimensional fluid flow in Ω (alternatively, using plane symmetry it can represent a membrane of infinite width in a three-dimensional fluid flow in $\Omega \times (-\infty, +\infty)$, or, using axial symmetry, a membrane ring in $\Omega \times (0, 2\pi)$). We denote by $\boldsymbol{A}(t) = \boldsymbol{\gamma}(t,0)$ and $\boldsymbol{B}(t) = \boldsymbol{\gamma}(t,1)$ the endpoints of $\Gamma(t)$, and s is the curvilinear coordinate along $\Gamma(t)$. We introduce $\boldsymbol{t} = \partial\boldsymbol{\gamma}/\partial s$ the tangent to $\Gamma(t)$, and $\boldsymbol{n}$ the normal such that $\boldsymbol{t} \times \boldsymbol{n} = 1$.

Let us assume that this thread or membrane is inextensible and has no resistance to bending, and that the fluid is incompressible and inertia-less. (The inertial case will be considered in the end of this section.) The fluid is set into motion by Dirichlet boundary conditions, $\boldsymbol{u} = \boldsymbol{u}_D$, imposed on $\Gamma_D = \partial\Omega$. The extension to Neumann boundary conditions is straightforward. The question of the necessity of prescribing additional boundary conditions to determine the behaviour of the thread or membrane will be addressed in this section as we expose the governing equations of the problem.

Over a time interval $(0,T)$, the problem writes:

Find $\boldsymbol{\gamma} \in C^0([0,T], H^{3/2}(0,1))$, $\boldsymbol{u} \in L^\infty\left(0,T, V^{\mathrm{div}}(\boldsymbol{u}_D,t)\right)$, such that:

$$J(\boldsymbol{u}(t)) = \min_{\boldsymbol{v}\in V^{\mathrm{div}}(\boldsymbol{u}_D,t)} J(\boldsymbol{v}) \qquad\qquad \text{a.e. } t \in [0,T],$$

$$\boldsymbol{\gamma}(t,s) = \boldsymbol{\gamma}_0(s) + \int_0^t \boldsymbol{u}(\tau, \boldsymbol{\gamma}(\tau,s))\,\mathrm{d}\tau, \quad \forall (t,\ s) \in [0,T] \times [0,1],$$

with

$$\Gamma(t) = \{ \boldsymbol{\gamma}(t, s), \ s \in (0, 1) \} ,$$

$$V^{\mathrm{div}}(\boldsymbol{u}_D, t) = \Big\{ \boldsymbol{v} \in H^1(\Omega)^2, \ \boldsymbol{v} \big|_{\Gamma(t)} \in H^{3/2}(\Gamma(t))^2, \ \boldsymbol{v} = \boldsymbol{u}_D \ \text{on} \ \Gamma_D,$$

$$\mathrm{div}\, \boldsymbol{v} = 0 \ \text{in} \ L^2(\Omega), \ \ \mathrm{div}_s\, \boldsymbol{v} = 0 \ \text{in} \ Z'(t) \Big\} ,$$

and

$$J(\boldsymbol{v}) = \int_\Omega |\mathbf{D}(\boldsymbol{v})|^2 \, \mathrm{d}V,$$

where $\mathbf{D}(\boldsymbol{v}) = \frac{1}{2} \left(\mathbf{grad}\, \boldsymbol{v} + (\mathbf{grad}\, \boldsymbol{v})^{\mathrm{T}} \right)$ is the rate-of-strain tensor, and the integration variable is $\mathrm{d}V = \mathrm{d}x\, \mathrm{d}y$ in plane symmetry, and $\mathrm{d}V = r\, \mathrm{d}r\, \mathrm{d}z$ in axial symmetry. (In that case, the functional spaces are understood as weighted Sobolev spaces, see [3]). The surface divergence operator is defined as $\mathrm{div}_s\, \boldsymbol{v} = \mathrm{div}\, \boldsymbol{v} - ((\mathbf{grad}\, \boldsymbol{v})\boldsymbol{n}) \cdot \boldsymbol{n}$. The functional space $Z'(t)$ is defined on $\Gamma(t)$ and will be characterised in the sequel. Note that in this particular case, no non-dimensional group arises when deriving these equations.

When $\Gamma(t)$ is known, this problem is equivalent to finding a saddle point $(\boldsymbol{u}; p, \zeta) \in V(\boldsymbol{u}_D) \times Q \times Z(t)$ of the Lagrangian function [2]:

$$\mathcal{L}(\boldsymbol{v}; q, \xi) = \int_\Omega |\mathbf{D}(\boldsymbol{v})|^2 \, \mathrm{d}V - \int_\Omega q\, \mathrm{div}\, \boldsymbol{v}\, \mathrm{d}V - \int_{\Gamma(t)} \xi\, \mathrm{div}_s\, \boldsymbol{v}\, \mathrm{d}A, \qquad (2.1)$$

with $\mathrm{d}A = \mathrm{d}s$ or $\mathrm{d}A = r\mathrm{d}s$ respectively in plane and axial symmetries. We have introduced the spaces :

$$V(\boldsymbol{v}_D) = \left\{ \boldsymbol{v} \in H^1(\Omega)^2, \ \boldsymbol{v} = \boldsymbol{v}_D \ \text{on} \ \Gamma_D \right\} ,$$

$$Q = \left\{ q \in L_0^2(\Omega) \right\} ,$$

and $Z(t) \subset H^{1/2}(\Gamma(t))$, the dual of $Z'(t)$, may have to include boundary conditions for ζ. These boundary conditions will be detailed in the sequel. The Lagrange multipliers p and ζ are respectively the pressure in the fluid and the tension in the membrane.

A saddle-point is characterised by the weak formulation:

$$\int_\Omega 2\mathbf{D}(\boldsymbol{u}) : \mathbf{D}(\boldsymbol{v}) \, \mathrm{d}V - \int_\Omega p\, \mathrm{div}\, \boldsymbol{v}\, \mathrm{d}V - \int_{\Gamma(t)} \zeta\, \mathrm{div}_s\, \boldsymbol{v}\, \mathrm{d}A = 0 \qquad \forall \boldsymbol{v} \in V(\boldsymbol{0})$$

$$- \int_\Omega q\, \mathrm{div}\, \boldsymbol{u}\, \mathrm{d}V = 0 \qquad \forall q \in Q$$

$$- \int_{\Gamma(t)} \xi\, \mathrm{div}_s\, \boldsymbol{u}\, \mathrm{d}A = 0 \qquad \forall \xi \in Z(t)$$

A generalisation of Green's formula for curved boundaries (e.g. [4]) can be formally applied to the boundary integrals above, expliciting the operator div_s. Note that this introduces a source term when $\Gamma(t)$ is curved (denoting κ its curvature):

$$\int_{\Gamma(t)} \xi\, \mathrm{div}_s\, \boldsymbol{v}\, \mathrm{d}A = - \int_{\Gamma(t)} \left(\frac{\partial \xi}{\partial s}\boldsymbol{t} + \kappa\xi\boldsymbol{n} \right) \cdot \boldsymbol{v}\, \mathrm{d}A + [\xi\boldsymbol{v} \cdot \boldsymbol{t}]_{\boldsymbol{A}(t)}^{\boldsymbol{B}(t)}. \qquad (2.2)$$

The above equation does not generally make sense for $\zeta \in H^{1/2}(\Gamma)$ and $\boldsymbol{v} \in H^{1/2}(\Gamma)^2$, for two (related) reasons: functions of $H^{1/2}(\Gamma)$ are not continuous, and the bilinear form $(\xi, v_t) \rightarrow \int_\Gamma (\partial \xi / \partial s) v_t \, \mathrm{d}A$ is not continuous on $H^{1/2}(\Gamma)^2$ [5, page 32]. This is related to the fact that the derivatives of functions in $H^{1/2}(\Gamma)$ are in the dual of $H_{00}^{1/2}(\Gamma)$ rather than in the dual of $H_0^{1/2}(\Gamma)$ [6, 7, lecture 33]. However, the physics of the problem dictates boundary conditions at points $\{\boldsymbol{A}, \boldsymbol{B}\} = \partial \Gamma(t)$ for these functions, which are, either, a fixed velocity or a fixed tension. For the sake of simplicity, we will only consider homogeneous cases of zero velocity or zero tension.

Zero-tension boundary conditions thus imply the choice $Z(t) = H_{00}^{1/2}(\Gamma(t))$. Then Eq. 2.2 makes sense if $\boldsymbol{v} \in L^\infty(\Gamma(t))^2$, and $\kappa \boldsymbol{n} = \partial^2 \boldsymbol{\gamma} / \partial s^2$ is in the dual of $H_{00}^{1/2}(\Gamma(t))$. A sufficient condition for these two requirements is that $\boldsymbol{u}$ and $\boldsymbol{v}$ be in $H^{3/2}(\Gamma(t))^2$. The case of zero-velocity conditions can also be treated, taking $Z(t) = H^{1/2}(\Gamma(t))$ and $\boldsymbol{u} \in H_0^{3/2}(\Gamma(t))^2 \subset H_{00}^{1/2}(\Gamma(t))^2$. Indeed, the product $\boldsymbol{u}\xi$ is in $H_{00}^{1/2}(\Gamma(t))$ (this can be verified using Hardy's inequality, see [7], and the fact that $H^{1/2}(\Gamma) \hookrightarrow L^8(\Gamma)$). Finally, one can apply a fixed velocity at one end of the moving boundary and a fixed tension at the other using the same ideas.

Note that the tension, unlike the pressure in Dirichlet boundary problems, is not defined up to a constant. The absolute value of the tension is either fixed by a boundary condition at a 'free' endpoint (one not in $\overline{\Gamma}_D$) or by the term $\kappa \xi \boldsymbol{n}$ if κ is not everywhere zero[1]. The value of the tension at a 'free' endpoint should be zero [8, p. 130], unless there is an external force other than hydrodynamic forces applied on that end.

We define:

$$a(\boldsymbol{u}, \boldsymbol{v}) = \int_\Omega 2\mathbf{D}(\boldsymbol{u}) : \mathbf{D}(\boldsymbol{v}) \, \mathrm{d}V$$

$$b(\boldsymbol{v}, q) = -\int_\Omega p \operatorname{div} \boldsymbol{v} \, \mathrm{d}V$$

$$c_{\Gamma(t)}(\boldsymbol{v}, \xi) = \int_{\Gamma(t)} \left(\frac{\partial \xi}{\partial s} \boldsymbol{t} + \kappa \xi \boldsymbol{n} \right) \cdot \boldsymbol{u} \, \mathrm{d}A$$

Using these notations, we rewrite the characterisation of the saddle-point $(\boldsymbol{u}; p, \zeta) \in V(\boldsymbol{u}_D) \times Q \times Z(t)$ defined in Eq. 2.1:

$$
\begin{aligned}
a(\boldsymbol{u}, \boldsymbol{v}) + b(\boldsymbol{v}, p) + c(\boldsymbol{v}, \zeta) &= 0 & \forall \boldsymbol{v} \in V(\boldsymbol{0}), & \quad (2.3\mathrm{a}) \\
b(\boldsymbol{u}, q) &= 0 & \forall q \in Q, & \quad (2.3\mathrm{b}) \\
c_{\Gamma(t)}(\boldsymbol{u}, \xi) &= 0 & \forall \xi \in Z(t), & \quad (2.3\mathrm{c})
\end{aligned}
$$

For a sufficiently regular solution, the saddle point problem is thus equivalent to the following strong formulation in terms of its momentum equation and the constraints:

---

[1] The case of a straight thread with both endpoints in $\overline{\Gamma}_D$ being either trivial, or ill-posed if a normal force is applied on the thread.

$$\begin{aligned}
\mathbf{grad}\, p - \mathbf{div}\, 2\mathbf{D}(\boldsymbol{u}) &= \mathbf{0} & &\text{in } \Omega \setminus \Gamma(t) \\
\operatorname{div} \boldsymbol{u} &= 0 & &\text{in } \Omega \\
\operatorname{div}_{\mathrm{s}} \boldsymbol{u} &= 0 & &\text{on } \Gamma(t)
\end{aligned}$$

$$\Gamma(t) = \left\{ \boldsymbol{\gamma}(t,s) = \boldsymbol{\gamma}_0(s) + \int_0^t \boldsymbol{u}(\tau, \boldsymbol{\gamma}(\tau))\, \mathrm{d}\tau,\ \forall s \in (0,1) \right\}$$

subject to the boundary condition:

$$\begin{aligned}
-[p]\boldsymbol{n} + [2\mathbf{D}(\boldsymbol{u})]\boldsymbol{n} &= \frac{\partial \zeta}{\partial s}\boldsymbol{t} + \kappa \zeta \boldsymbol{n} & &\text{on } \Gamma(t) \\
\boldsymbol{u} &= \boldsymbol{u}_D & &\text{on } \Gamma_D \\
\zeta(\boldsymbol{P}) &= 0 & &\text{for } \boldsymbol{P} \in \partial\Gamma(t) \setminus \overline{\Gamma}_D
\end{aligned}$$

where the notation $[\cdot]$ refers to the jump of a quantity accross the interface $\Gamma(t)$.

In the case when there is inertia, the energy variation term J needs to include kinetic energy of both the fluid and the thread, and becomes :

$$J(\boldsymbol{v}) = \operatorname{Re} \frac{\mathrm{d}}{\mathrm{d}t} \int_\Omega \boldsymbol{v}^2\, \mathrm{d}V + \operatorname{Re}_\Gamma \frac{\mathrm{d}}{\mathrm{d}t} \int_{\Gamma(t)} \boldsymbol{v}^2\, \mathrm{d}A + \int_\Omega |\mathbf{D}(\boldsymbol{v})|^2\, \mathrm{d}V,$$

where $\operatorname{Re} = \rho U L / \eta$ and $\operatorname{Re}_\Gamma = \lambda U / \eta$ are two Reynolds numbers associated with the fluid of surfacic density ρ and viscosity η, and the thread of lineic density λ and length L, for a typical velocity U. An initial condition for $\boldsymbol{u}$ must then be provided. The same procedure can be applied to impose the inextensibility of the thread.

Finally, let us note that any other volume or surface force can be easily taken into account in this setting, such as a bending rigidity [1].

3. Finite element discretisation. In order to have explicit meshes of both Ω and $\Gamma(t)$, and no interpolation between the spaces defined on these meshes, we first introduce an approximation of Γ_0:

$$\Gamma_h^0 = \left\{ e_i^0 = [\boldsymbol{x}_i^0,\, \boldsymbol{x}_{i+1}^0],\ \boldsymbol{x}_i^0 \in \Gamma(t), |e_i| < h,\ \forall i = 0, ..., N-1, \boldsymbol{x}_0^0 = \boldsymbol{A}^0, \boldsymbol{x}_N^0 = \boldsymbol{B}^0 \right\}$$

The finite element mesh $\mathcal{T}_h^0$ of Ω, composed of triangles of diameter smaller than h, is then defined such that all the edges e_i^0 are among the sides of the triangles. Being given an approximation $\boldsymbol{u}_h^n$ of the velocity field $\boldsymbol{u}$ at time t_n, a sequence of approximations of the moving interface $\Gamma(t)$ at time $t_{n+1} = t_n + \Delta t$ can be constructed as:

$$\Gamma_h^{n+1} = \left\{ e_i^{n+1} = e_i^n + \Delta t\, [\boldsymbol{u}_h^n(\boldsymbol{x}_i^n), \boldsymbol{u}_h^n(\boldsymbol{x}_{i+1}^n)],\ \forall i = 0, ..., N-1 \right\}. \tag{3.1}$$

and hence a triangulation $\mathcal{T}_h^{n+1}$ can be obtained either by remeshing or by advecting interior node with an ad-hoc mesh velocity $\boldsymbol{c}_h^n$, this latter option being known as the arbitrary Lagrangian–Eulerian technique [9]. Inextensibility allows to derive an upper bound in $O(h(1 + \Delta t)^n)$ for the length of the edges e_i^{n+1}, periodic remeshing of Ω_h^{n+1} and occasionnally of Γ_h^{n+1} are nevertheless necessary to ensure mesh quality. We define $\boldsymbol{c}_h^n \in X_h^n(\boldsymbol{u}_h^n) = V(\mathbf{0}) \cap \{\boldsymbol{v}_h \in P_1(\mathcal{T}_h^n), \boldsymbol{v}_h(\boldsymbol{x}_i^n) = \boldsymbol{u}_h^n(\boldsymbol{x}_i^n),\ \forall \boldsymbol{x}_i^n \in \Gamma_h^n,\ i = 0, ..., N-1\}$ as the solution of the problem:

$$\int_\Omega \mathbf{D}(\boldsymbol{c}_h^n) : \mathbf{D}(\boldsymbol{v}_h)\, \mathrm{d}V = 0 \qquad\qquad \forall \boldsymbol{v}_h \in X_h^n(\mathbf{0}). \tag{3.2}$$
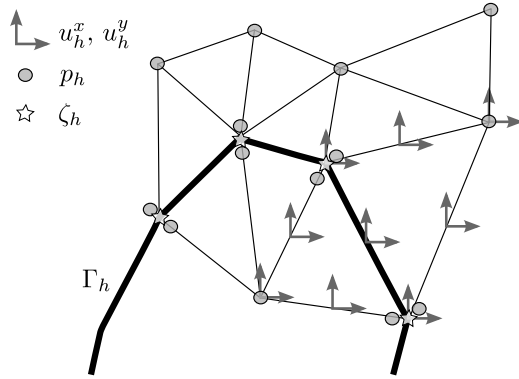
FIG. 3.1. *The choice of finite element spaces for a thread with no 'free' endpoint. Velocity $\boldsymbol{u}$ is continuous, quadratic by piece; pressure p linear by piece and continuous except accross the thread; and tension ζ is continuous, linear by piece (defined only on the thread). Velocity discretisation is shown for two elements only.*

We then introduce the finite element spaces $P_k(\mathcal{T}_h)$ of piecewise polynomial functions of degree k. We define $V_h^n(\boldsymbol{v}_{D,h}) = V(\boldsymbol{v}_{D,h}) \cap P_2(\mathcal{T}_h^n) \cap C^0(\Omega)$, and $Q_h^n = Q \cap P_1(\mathcal{T}_h^n) \cap C^0(\Omega \setminus \Gamma_h^n)$. The pressure approximation is thus taken continuous except accross the (approximation of the) interface. Because this discontinuity is thus localised, this does not break the Babuška–Brezzi condition [10] as far as the velocity–pressure pair is concerned.

Further, we introduce

$$Z_{m,h}^n = \left\{ \xi_h \in P_m(\Gamma_h^n), \xi_h(\boldsymbol{P}) = 0 \text{ for } \boldsymbol{P} \in \partial\Gamma_h^n \setminus \overline{\Gamma}_D \right\} \cap C^0(\Gamma_h^n),$$

whose degree m has to be determined such that the Babuška–Brezzi condition holds for the composite Lagrange multiplier formed of pressure and tension. It turns out empirically that, when the contiuous space is $Z(t) = H^{1/2}(\Gamma(t))$, using $m = 1$ (which correponds to the discretisation pictured in Fig. 3.1) leads to a stable scheme. This scheme is shown to converge to the analytical solution on an example in section 4.1. Thus this seems to be the appropriate choice when the interface has no 'free' endpoint (i.e., when $\partial\Gamma(t) \setminus \overline{\Gamma}_D = \varnothing$).

However, in the case of an interface with one 'free' endpoint, where a boundary condition must be imposed on the tension (e.g., when $Z(t) = H_{00}^{1/2}(\Gamma(t))$), oscillations appear in the velocity field on the interface, close to this 'free' endpoint. From a discrete viewpoint, these correspond to modes in the kernel of the inextensibilty operator, due to the deletion of the degree of freedom corresponding to the Dirichlet boundary condition on the tension. For Γ_0 with $\kappa = 0$ (straight segment), it is in fact quite easy to construct elements $\tilde{\boldsymbol{u}}_h$ of V_h^0 such that $\text{div}_s\, \tilde{\boldsymbol{u}}_h \neq 0$ but $c_{\Gamma_h^n}(\tilde{\boldsymbol{u}}_h, \xi_h) = 0$ for all $\xi_h \in Z_{1,h}^0$. The interpretation is thus that the $P_1(\Gamma_h)$ test-space is too small to enforce inextensibility close to the endpoint of the moving boundary. Adding an extra degree of freedom for the tension locally in the last edge element does not help this behaviour, but only reproduces the same problem in the penultimate edge element. Using $m = 2$ in turn, that is, quadratic-by-piece tension, allows to enforce inextensibility, but results in a spurious oscillation mode at the mid-edge values of the tension. It is thus not obvious empirically, whether an adequate choice of spaces exists that would verify the Babuška–Brezzi condition. However, in the case $m = 2$, oscillations

in tension can be filtered a posteriori by projection to $Z_{1,h}^n$ [10]. This strategy was employed in sections 4.2 and 4.3.

A sequence $(\Gamma_h^n, \boldsymbol{u}_h^n, p_h^n, \zeta_h^n)_n$ is then obtained by iterating resolution steps of Eq. 2.3 and advection steps of Eq. 3.1:

a) Calculate $\kappa_h^n \boldsymbol{n}_h$ on macro-edge boundary elements e of Γ_h^n using a quadratic interpolation $\tilde{\gamma}_e^n \in P_2(e)$.

b) Find $(\boldsymbol{u}_h^n, p_h^n, \tilde{\zeta}_h^n) \in V_h^n(\boldsymbol{u}_{D,h}) \times Q_h^n \times Z_{m,h}^n$, such that, for all $(\boldsymbol{v}_h, q_h, \xi_h) \in V_h^n(\boldsymbol{0}) \times Q_h^n \times Z_{m,h}^n$:

$$a(\boldsymbol{u}_h^n, \boldsymbol{v}_h) + b(\boldsymbol{v}_h, p_h^n) + c_{\Gamma_h^n}(\boldsymbol{v}_h, \zeta_h^n) = 0, \qquad (3.3\text{a})$$

$$b(\boldsymbol{u}_h^n, q_h) = 0, \qquad (3.3\text{b})$$

$$c_{\Gamma_h^n}(\boldsymbol{u}_h^n, \xi_h) = 0. \qquad (3.3\text{c})$$

c) If $m = 2$, find $\zeta_h^n \in Z_{1,h}^n$ such that

$$\int_{\Gamma_h^n} (\zeta_h^n - \tilde{\zeta}_h^n)\xi_h \, \mathrm{d}A = 0 \qquad \forall \xi_h \in Z_{1,h}^n,$$

else set $\zeta_h^n = \tilde{\zeta}_h^n$.

d) Calculate the mesh advection velocity $\boldsymbol{c}_h^n$ using Eq. 3.2.

e) Calculate mesh Ω_h^{n+1} by advection of Ω_h^n by $\Delta t \, \boldsymbol{c}_h^n$, remesh if necessary.

Step b is the problem considered by Fortin ang Glowinski [2], and is solved using an augmented Lagrangian technique with Uzawa algorithm.

When Re > 0, we make use of the method of characteristics to calculate the material derivative, as described for both the Lagrangian and ALE methods in [11]. An extra term then appears in the right hand side of Eq. 3.3a (and also in the right hand side of Eq. 3.3c in the case $\mathrm{Re}_\Gamma > 0$).

4. Numerical tests.

4.1. Swollen vesicle in Stokes flow. A spherical object, filled with an incompressible fluid and bounded with an inextensible membrane is rendered undeformable by the combination of these two constraints. This can easily be seen from the fact that any volume-preserving deformation of a sphere increases its area. As a result, such a vesicle must behave as a hard sphere, possibly with surface flow at the boundary since the membrane is fluid. This surface flow may be quenched by choosing a setup with appropriate symmetries, so that the vesicle will behave as a hard sphere with no-slip boundary conditions.

Thus it appears that a demanding test of our method is to calculate the permanent flow generated by the fall or rise of a buoyant vesicle with a fluid membrane in a fluid at rest, see Fig. 4.1. In the frame of the vesicle, this problem writes,

Find $\boldsymbol{u}$, p and ζ such that:

$$\mathbf{grad}\, p - \mathbf{div}\, 2\mathbf{D}(\boldsymbol{u}) = -\rho \boldsymbol{e}_z \qquad \text{in } (\mathbb{R}^+ \times \mathbb{R}) \setminus \Gamma,$$

$$\mathrm{div}\, \boldsymbol{u} = 0 \qquad \text{in } \mathbb{R}^+ \times \mathbb{R},$$

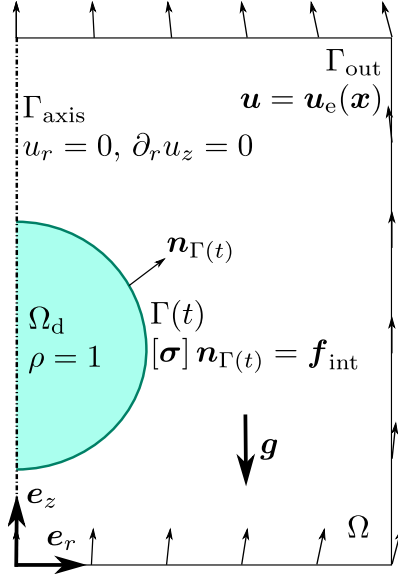$$\mathrm{div}_\mathrm{s}\, \boldsymbol{u} = 0 \qquad \text{on } \Gamma,$$

FIG. 4.1. *Boundary conditions for the swollen vesicle in Stokes flow problem. The flow imposed through the boundary condition counterbalances exactly the gravity force acting on the object. Through the saddle-point approach, pressure and surface forces are calculated that enforce the undeformability of the subdomain Ω_d.*
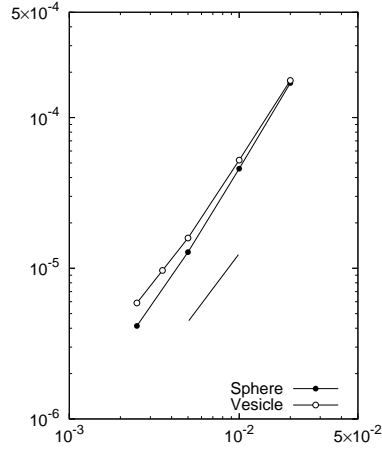

FIG. 4.2. *Error in H^1 norm as a function of h for the direct resolution of the falling sphere problem with $\boldsymbol{u} = \boldsymbol{0}$ on Γ and for the undeformable vesicle problem. The line indicates the $h^{3/2}$ slope.*

subject to the boundary conditions:

$$-[p]\boldsymbol{n} + [2\mathbf{D}(\boldsymbol{u})]\boldsymbol{n} = \frac{\partial \zeta}{\partial s}\boldsymbol{t} + \kappa\zeta\boldsymbol{n} \qquad \text{on } \Gamma,$$

$$\boldsymbol{u} \to u_0\boldsymbol{e}_z \qquad \text{as } \sqrt{r^2 + z^2} \to \infty,$$

$$\left.\begin{aligned}\boldsymbol{u} \cdot \boldsymbol{e}_r &= 0 \\ \frac{\partial \boldsymbol{u} \cdot \boldsymbol{e}_z}{\partial r} &= 0\end{aligned}\right\} \text{on } \Gamma_{\text{axis}},$$
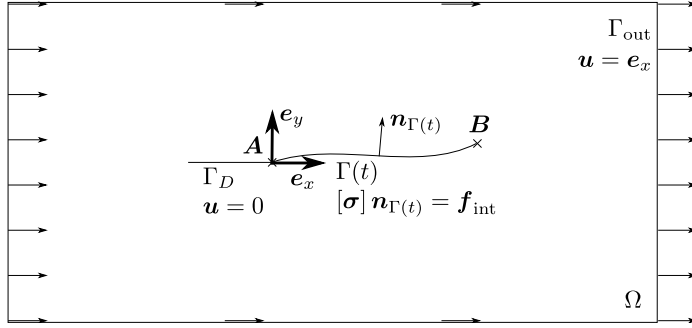
FIG. 4.3. *Geometry and boundary conditions for the flow past a flag problem. The flow past a plate can be simulated when the curve $\Gamma(t)$ is a straight segment aligned with $\boldsymbol{e}_x$.*

ρ being the buoyancy, set to one in Ω_d and zero elsewhere. No boundary condition is necessary for the tension, since the endpoints of Γ are on the axis Γ_axis and have zero velocity in the direction $\boldsymbol{e}_r$, which is tangent to the membrane at these points. Here the problem is written as static, because we will see that it results in $\boldsymbol{u} = 0$ on the membrane Γ provided that u_0 is chosen such that gravity and drag forces balance.

Indeed, because of the axial symmetry of the problem, the membrane is actually at rest in the frame of the mass centre of the vesicle (no tangential flow), and thus the vesicle behaves as a solid sphere. Because in addition there is no shear source in the fluid inside the vesicle, it is at rest and the problem reduces to the flow generated by a buoyant inelastic solid sphere. This problem consists of the problem above stated in Ω_e only and with boundary condition $\boldsymbol{u} = 0$ on Γ and has an analytical solution [12],

$$\boldsymbol{u} \cdot \boldsymbol{e}_R = u_R = u_0 \sin \Psi \left(1 - \frac{3}{2R} + \frac{1}{2R^3} \right),$$

$$\boldsymbol{u} \cdot \boldsymbol{e}_\Psi = u_\Psi = u_0 \cos \Psi \left(1 - \frac{3}{4R} - \frac{1}{4R^3} \right),$$

written in spherical coordinates with $R = \sqrt{r^2 + z^2}$ and $\Psi = \tan^{-1} \frac{z}{r}$, $\boldsymbol{e}_R$ and $\boldsymbol{e}_\Psi$ being the corresponding basis vectors. This also yields the drag force, and hence the value of u_0 balancing the gravity force, $u_0 = 2/9$.

Using this analytical solution, we can prescribe a boundary condition at a finite distance from the sphere ($\Omega = (0, 10) \times (-10, 10)$). We simulate the problem with four meshes of different refinement, Ω_h with $h \in \{2h_0, h_0, h_0/2, h_0/4\}$, which are obtained by refining or coarsening the original mesh Ω_{h_0} of approximately 2500 elements. The H^1 error $\|u_e - u_h\|_1$ is found to decrease as $O(h^{1.5})$ (Fig. 4.2), which corresponds to the expected rate of convergence. The sub-optimality of this rate compared to $O(h^2)$ convergence of Stokes flow in a polygonal domain is due to the absence of an isoparametric implementation of the finite elements method. The method is seen to be nearly as accurate as the direct implementation of a solid sphere.

4.2. Flow past a plate. We now turn to the case when the curve $\Gamma(t)$ has one 'free' end, but still in conditions in which there will be no time evolution of $\Gamma(t)$ because inextensibility forces balance hydrodynamic forces. This is the case of a 'flag', or a piece of thread in a two-dimensional flow such as a soap film [13] if the thread is initially aligned with the flow direction. This setup simulates the flow past a plate, a
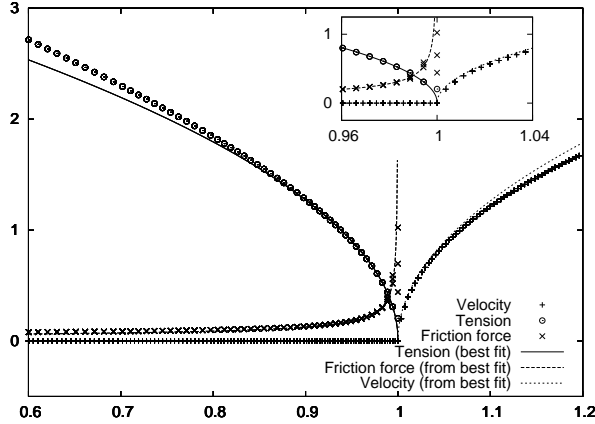
FIG. 4.4. *Comparison of the numerical solution for the tension $\zeta_h(x, 0)$, velocity $u_h^x(x, 0)$ and friction force $\frac{\partial u_h^x}{\partial y}(x, 0^+)$ on the line $y = 0$ around point $\boldsymbol{B} = (1, 0)^{\mathrm{T}}$, with the asymptotic behaviours $\zeta \sim a\sqrt{1-x}$, $u^x \sim \frac{a}{4}\sqrt{\max\{x - 1, 0\}}$ and $\frac{\partial u^x}{\partial y}(x, 0^+) = -\frac{\partial \zeta}{\partial x} \sim \frac{a}{2\sqrt{1-x}}$. Parameter a was identified by best fit of ζ_h over the range $x \in [0.9, 0.999]$ and thence used for all the comparisons. The friction stress is multivalued at $\boldsymbol{B}$, however its limit for $\boldsymbol{x} = (1 - \varepsilon, 0)$ is close to the asymptotic value. The tension should tend to 0 at $\boldsymbol{A}$, this is a boundary condition for the P_2 field $\tilde{\zeta}_h$, but is not verified pointwise by its projection ζ_h on P_1 (see insert). However, the value is correct for degrees of freedom at $x < 1$.*

problem equivalent to the Stokes 'stick-slip' problem, for which an asymptotic solution is known [14, 15].

Fig. 4.3 describes the geometry and boundary conditions, with $\overline{\Omega} = [-5, 5] \times [-2 \times 2]$ and $\partial\Omega = \Gamma_{\mathrm{out}} \cup \Gamma_D$. The initial condition is $\gamma_0(s) = (s, 0)^{\mathrm{T}}$, and our analysis states that at later times, $\gamma(t, s) = \gamma_0(s)$. We test the numerical implementation with respect to this result and the asymptotic solution of the Stokes 'stick-slip' problem.

We find empirically that the discrete inf-sup condition is violated for the choice $(\boldsymbol{u}_h, p_h, \zeta_h) \in V_h(\boldsymbol{u}_{D,h}) \times Q_h \times Z_{1,h}$: the velocity on Γ_h oscillates in a neighbourhood of point $\boldsymbol{B}$. Using a Lagrange multiplier $\tilde{\zeta}_h \in Z_{2,h}$ these velocity oscillations disappear. Oscillations however appear on $\tilde{\zeta}_h$, which can be filtered thanks to the projection method described in Section 3 to obtain the tension $\zeta_h \in Z_{1,h}$. In Fig. 4.4 we compare the numerical solution obtained with our scheme to the asymptotic solution around point $\boldsymbol{B}$. It is seen that the numerical solution verifies closely this asymptotic solution. In particular, the velocity on Γ_h is zero up to floating point operations error (10^{-11}), and increases sharply in the neighbourhood of the flag (see Fig. 4.5). The numerical scheme is thus successful at describing a truly inextensible thread in conditions where the stress diverges at the endpoint.

4.3. Flag in a high Reynolds-number flow. With the same initial conditions as in the previous section, we find that the flow can be unstable for a finite value of the Reynolds number. Such an instability is found experimentally for a filament in a twodimensional fluid flow [13], although it is generally believed that it is due to the interplay of fluid inertia and (bending) elasticity of the filament [16]. Here there is no
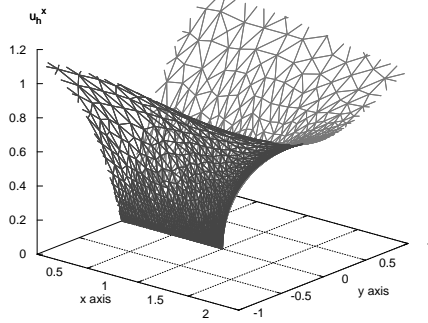
FIG. 4.5. *Approximation u_h^x of the velocity in the neighbourhood of the flag. Visualisation uses $P_1 - iso - P_2$ approximation.*

such elasticity term, and we find that the shear generated by viscous friction on an inextensible filament can lead to an instability.

The geometry and boundary conditions of the problem are again those in Fig. 4.3, and the strong formulation of the problem considered writes:

Find $\boldsymbol{u}, p$ and ζ such that:

$$\mathrm{Re}\left(\frac{\partial \boldsymbol{u}}{\partial t} + \boldsymbol{u} \cdot \mathbf{grad}\,\boldsymbol{u}\right) + \mathbf{grad}\,p - \mathbf{div}\,2\mathbf{D}(\boldsymbol{u}) = -\rho\boldsymbol{e}_z \qquad \text{in } \Omega \setminus \Gamma(t)$$

$$\mathrm{div}\,\boldsymbol{u} = 0 \qquad \text{in } \Omega$$

$$\mathrm{div}_{\mathrm{s}}\,\boldsymbol{u} = 0 \qquad \text{on } \Gamma$$

subject to the boundary conditions:

$$\mathrm{Re}_\Gamma\left(\frac{\partial \boldsymbol{u}}{\partial t} + \boldsymbol{u} \cdot \mathbf{grad}\,\boldsymbol{u}\right) - [p]\boldsymbol{n} + [2\mathbf{D}(\boldsymbol{u})]\boldsymbol{n} = \frac{\partial \zeta}{\partial s}\boldsymbol{t} + \kappa\zeta\boldsymbol{n} \quad \text{on } \Gamma(t)$$

$$\boldsymbol{u} = \boldsymbol{e}_x \qquad \text{on } \Gamma_{\mathrm{out}}$$

$$\boldsymbol{u} = \mathbf{0} \qquad \text{on } \Gamma_D$$

and initial conditions $\gamma_0(s) = (s, 0)^{\mathrm{T}}$ and $\boldsymbol{u}(0) = \boldsymbol{u}_0$, the solution of the zero-Reynolds problem solved in Section 4.2.

In this example, we choose $\mathrm{Re} = \mathrm{Re}_\Gamma = 10^3$. The evolution of $\Gamma_h(t)$ is shown on Fig. 4.6. It is found that perturbations of the order of the numerical error are sufficient to trigger oscillations that grow to first order amplitude. These oscillations are the topic of a forthcoming paper.

5. Conclusions. We develop and demonstrate a novel numerical method for the simulation of problems involving a constraint on a moving boundary, in the present case, the inextensibility constraint. This is done by making use of a surface Lagrange
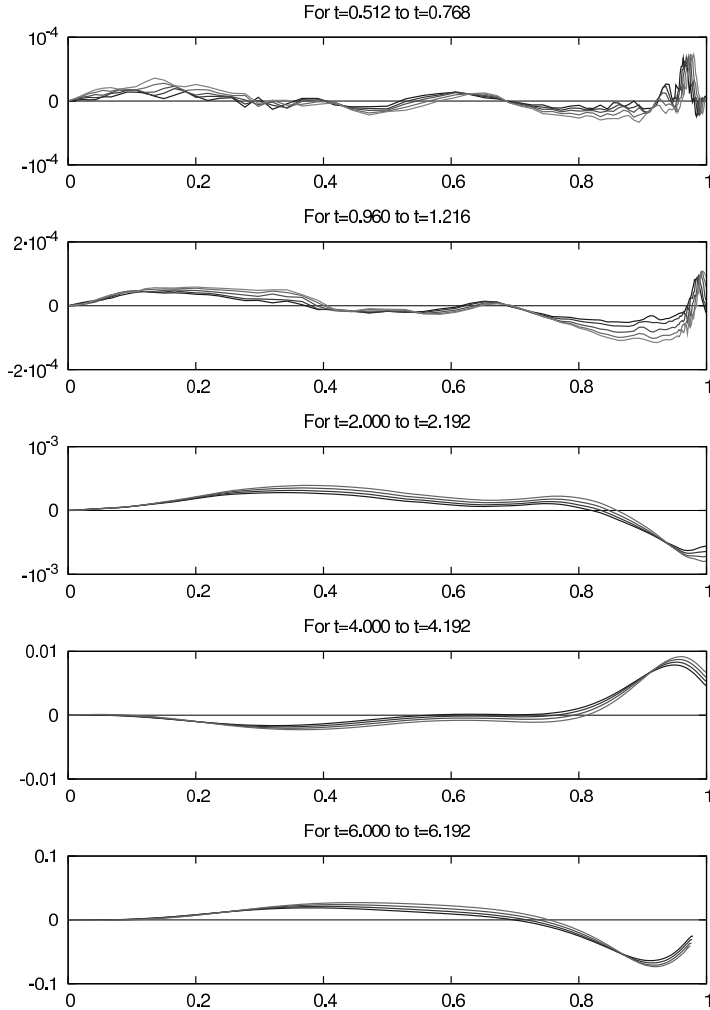
FIG. 4.6. *Time evolution of the filament $\Gamma_h(t)$ for $\mathrm{Re} = \mathrm{Re}_\Gamma = 10^3$. The y-axis is magnified differently in each plot, there is no magnification in the last one. Different gray levels correspond to different successive instants, from dark to light gray. At $t \simeq 0.5$, small random perturbations are seen, which amplify and result in travelling waves of growing amplitudes for $t \gtrsim 2$. For $t \simeq 6$, the amplitude of these waves is of the same order as the filament length.*

multiplier (called *tension*), which allows to enforce accurately the inextensibility constraint locally on the thread or membrane. A variational formulation of this constrained problem is given, using a saddle-point approach in an analogous manner as for the incompressibility constraint. Here, however, the tension force associated with the Lagrange multiplier is a surfacic force applied on the inextensible boundary. Because this boundary may be curved, one finds that in addition to the tangential surfacic tension force, which is the surface gradient of the tension, a normal component arises which involves the local value of the tension and of the curvature. This differs with the case of bulk incompressibility, where only the gradient of the corresponding Lagrange multiplier (pressure) appears. The boundary conditions specific to the inextensible moving boundary are explicited in the context of the variational formulation

of the saddle-point problem, they are in agreement with the physical consideration that at the endpoints of the boundary, either the tension (corresponding to a point force) or the tangential velocity must be imposed.

To take the best advantage of this method, which allows to enforce that the velocity on the moving boundary verifies the inextensibility constraint up to roundoff error, it is better not to interpolate the value of velocity over a non-matching bulk mesh, as would be done in an immersed boundary or a level-set method. Using a Lagrangian or an arbitrary Lagrangian–Eulerian (ALE) method allows to have a bulk mesh that includes the moving boundary's mesh in the set of its edges. Hence, there is no need for interpolation and the inextensibility force is actually treated as a boundary condition rather than approximated by a bulk force. This allows our implementation to yield sharp velocity profiles as in the example in Fig. 4.5. It is shown in this and other examples that the combination of the Lagrange multiplier approach and an ALE method based on finite elements yields a very accurate and highly robust numerical method, allowing to focus on stiff problems of fluid-structure interactions: in the swollen vesicle example, the combination of incompressiblity and inextensibility constraints maintain the shape of the vesicle like an inflated ball; in the 'flag' example, the structure interacts with a high-Reynolds number fluid flow.

Some questions arise however which are not addressed within the scope of this paper. Indeed, it is well known that mixed methods require a compatibility condition between the finite element space of the Lagrange multiplier and the one of the original variable. Here, it is found empirically that, if the moving boundary forms a closed loop, or has both endpoints fixed by means of a Dirichlet boundary condition on the velocity, the surfacic Lagrange multiplier can be taken continuous linear by piece ($P_1(\Gamma_h)$) when the velocity is continuous quadratic by piece ($P_2(\Omega_h)$). However, this is not the case anymore when at least one of the endpoints of the moving boundary is free to move, that is, when the boundary condition is imposed on tension rather than velocity. In that case, we find that a $P_1(\Gamma_h)$ test-space is too small to enforce inextensibility close to the endpoint of the moving boundary, as there exist discrete velocity fields which do not verify the (continuous) inextensibility constraint but are in the kernel of the corresponding discrete surface divergence operator. Employing a $P_2(\Gamma_h)$ test-space and filtering the resulting Lagrange multiplier to obtain the tension did circumvent this problem. It remains an open question whether in this case there exists an adequate choice of spaces that would verify the Babuška–Brezzi condition.

Finally, we would like to stress that there are many physical situations of interest in which the strong points of this method could prove decisive. Indeed, any penalty method implies to choose globally an extensibility modulus. Thus, regions of strong sollicitation will extend proportionately more in a penalty method, which will not be the case using a Lagrange multiplier approach. Yet, a physical situation as common and simple as a filament extended by a flow field, fixed by one of its ends, exhibits a sollicitation that goes to infinity at its free end. It is thus crucial to pay attention to this issue.

REFERENCES

[1] W. Helfrich. Elastic properties of lipid bilayers: Theory and possible experiments. *Z. Naturforsch.*, 28C:693–793, 1973.

[2] M. Fortin and R. Glowinski. *Augmented Lagrangian methods, applications to the numerical solution of boundary value problems*. Elsevier Science, Amsterdam, 1983.

[3] A. Kufner. *Weighted Sobolev Spaces*, volume 31 of *Teubner-Text zur Mathematik*. Teubner-Verlag, Leipzig, 1980.

[4] A. Laadhari, C. Misbah, and P. Saramito. On the equilibrium equation for a generalized biological membrane energy by using a shape optimization approach. *submitted*, 2009.

[5] P. Grisvard. *Elliptic problems in non-smooth domains*. Pitman, London, 1985.

[6] J.-L. Lions and E. Magenes. *Problèmes aux limites non homogènes, Vol. 1*. Number 17 in Travaux et Recherches Mathématiques. Dunod, 1968.

[7] L. Tartar. *An introduction to Sobolev spaces and interpolation spaces*, volume 3 of *Lecture Notes of the Unione Matematica Italiana*. Springer, Berlin, Heidelberg, 2007.

[8] F. Divet. *Fluctuations d'une membrane en interaction avec un champ diffusif*. PhD thesis, Université Joseph Fourier, Grenoble I, 2001.

[9] C. W. Hirt, A. A. Amsden, and J. L. Cook. An arbitrary Lagrangian–Eulerian computing method for all flow speeds. *J. Comput. Phys.*, 135:203–216, 1997. reprinted from J. Comput. Phys., 14:227, 1974.

[10] F. Brezzi and M. Fortin. *Mixed and hybrid finite elements methods*. Springer-Verlag, New-York, 1991.

[11] J. Étienne, E. J. Hinch, and J. Li. A Lagrangian–Eulerian approach for the numerical simulation of free-surface flow of a viscoelastic material. *J. Non-Newtonian Fluid Mech.*, 136:157–166, 2006.

[12] H. Lamb. *Hydrodynamics*. Dover, New-York, 1945.

[13] J. Zhang, S. Childress, A. Libchaber, and M. Shelley. Flexible filaments in a flowing soap film as a model for one-dimensional flags in a two-dimensional wind. *Nature*, 408:835–838, 2000.

[14] S. Richardson. A 'stick-slip' problem related to the motion of a free jet at low Reynolds numbers. *Math. Proc. Cambridge Phil. Soc.*, 67:477–489, 1970.

[15] G.C. Georgiou, L.G. Olson, W.W. Schultz, and S. Sagan. A singular finite element for Stokes flow: the stick-slip problem. *Int. J. Numer. Methods Fluids*, 9:1353–1367, 1989.

[16] M. Argentina and L. Mahadevan. Fluid-flow-induced flutter of a flag. *Proc. Natl. Acad. Sci. USA*, 102:1829–1834, 2005.